Expanded View Figures

Figure EV1. Q modification-related behavioral changes.

A Representative track record of wt and Q1 mice subjected to open-field test.

B, C Total distance traveled (B) and distance traveled in the center (C) are shown. Statistical significance was analyzed by two-tailed unpaired *t*-test. Data points are shown as ±SEM; ($n = 6$).

D–F The graphs show the locomotion duration, distance, and speed measured in home cage observation test. Statistical significance was analyzed by two-tailed unpaired *t*-test. Data points are shown as ±SEM; ($n \geq 14$).

G Visual navigation capacities were measured before the MWM training. The animals were directed to the escape platform with the help of visual cues around the maze and a flagged platform. Each dot represents an individual. Error bars demonstrate ±SEM ($n = 6$; 4 trials per each replicate).

H Representative swimming paths on day 2 and day 10 of MWM test. Spatial learning was tested in 5- to 6-month-old mice by the MWM test. The mice were left for 90 s in a water-filled alley with an invisible platform as a motivation to escape. The swimming was recorded and tracked with Sygnis tracker. Red lines indicate the swimming path.

I The escape latency was determined as the time spent until an animal finds the platform within 90 s and plotted as the learning curve over 10 consecutive days. Data points represent ±SEM; ($n = 6$; 4 trials within each biological replicate per day). Statistical significance was analyzed by two-way ANOVA followed by Benjamini and Hochberg *post hoc* test. *P*-values for genotype effect and at individual time points are indicated in the curves.

J The number of success refers to the number of times an animal finds the platform within 90 s trial. Statistical significance was analyzed by beta regression. The effect of sex on overall genotypes; *P*-value = 0.0000344. Significant *P*-values for genotype effect (Q1 versus wt) for both male and female are indicated. ($n = 6$; 4 trials within each biological replicate per day).

K Representative swimming paths on day 12 (probe trial) of the MWM test. Red lines indicate the swimming path.

L Percentage of time each animal spent in each quadrat during the probe trial (day 12) in the MWM test. The statistical effect of the genotype on the time in quadrant 1 (which had the platform) was calculated using the Wilcoxon rank-sum test (two-sided). Data points are shown as ±SEM; ($n = 6$).

M Percentage of time that each animal group spent in each quadrat during the probe trial (day 12) in the MWM test. The target quadrant 1 is indicated in blue.

Data information: Q1, *Qtrt1* knockout mouse; wt, wild-type mouse. **P*-value < 0.05, ***P*-value < 0.01, ****P*-value < 0.001.

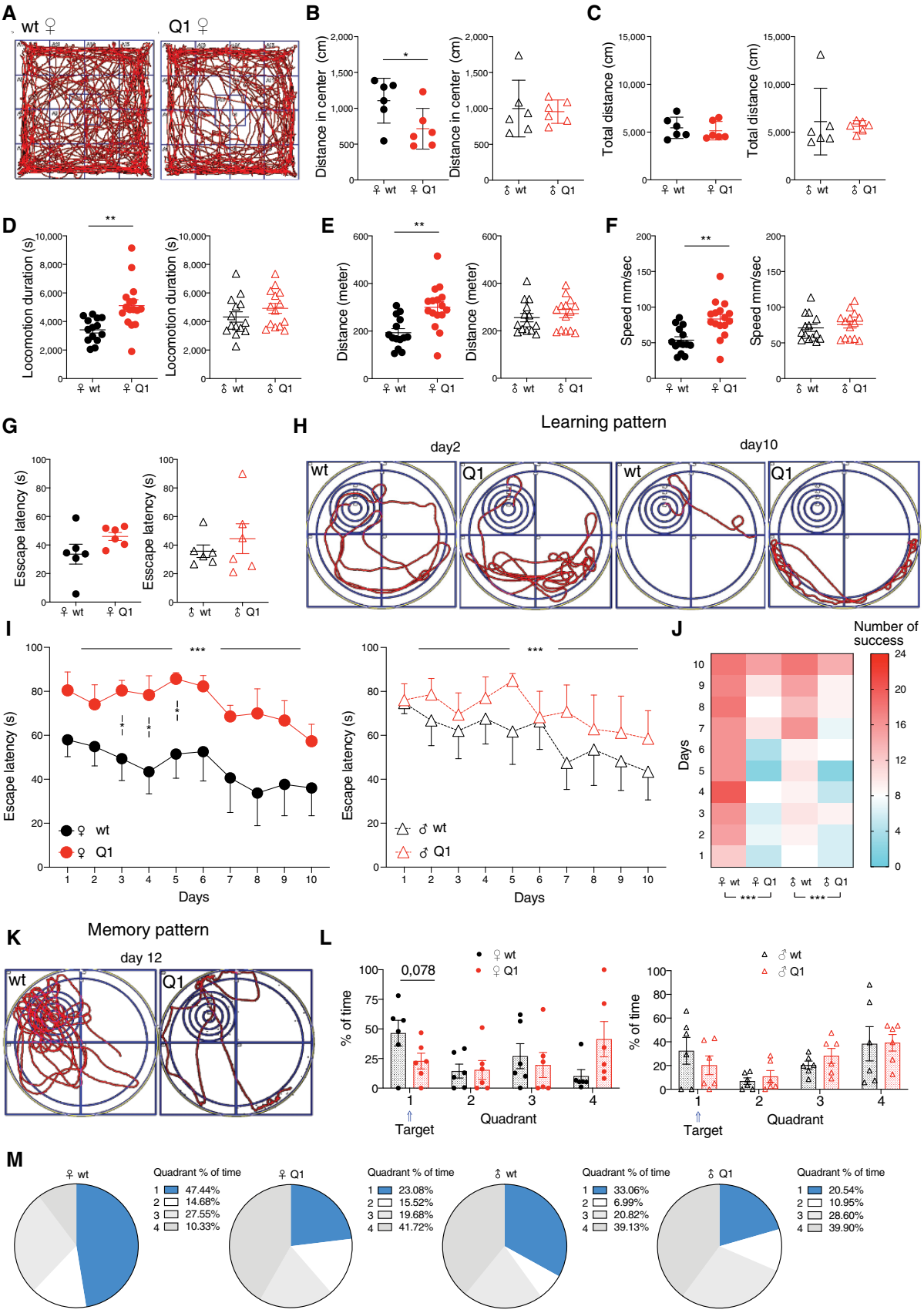

Figure EV1.

Figure EV2. Gross brain morphology and glial cells are mostly unaffected in Q1 mice.

A Nissl staining of brain coronal sections from 6- to 7-month-old mice. Neurons are stained in violet–blue.
B Brain weight of 6- to 7-month-old mice. Error bars indicate ±SD (n = 6, 3 males and 3 females).
C Immunostainings and quantification of astrocyte (GFAP) and microglia (IBA1) in the 7-month-old hippocampi. Green cells: GFAP, violet cells: IBA1, and blue: DAPI. Scale bar 100 μm. The number of positive cells was counted manually using ImageJ. Error bars indicate ±SD; ($n \geq 6$).
D RNA *in situ* hybridization identifying oligodendrocytes (*Plp1*) in the 7-month-old hippocampi. Green: *Plp1*, and blue: DAPI. Scale bar 100 μm. The number of positive cells was counted manually using ImageJ. Error bars indicate ±SD ($n \geq 8$).
E TUNEL assay showing similar cell death in the wt and Q1 hippocampus.

Data information: Q1, *Qtrt1* knockout mouse; wt, wild-type mouse.

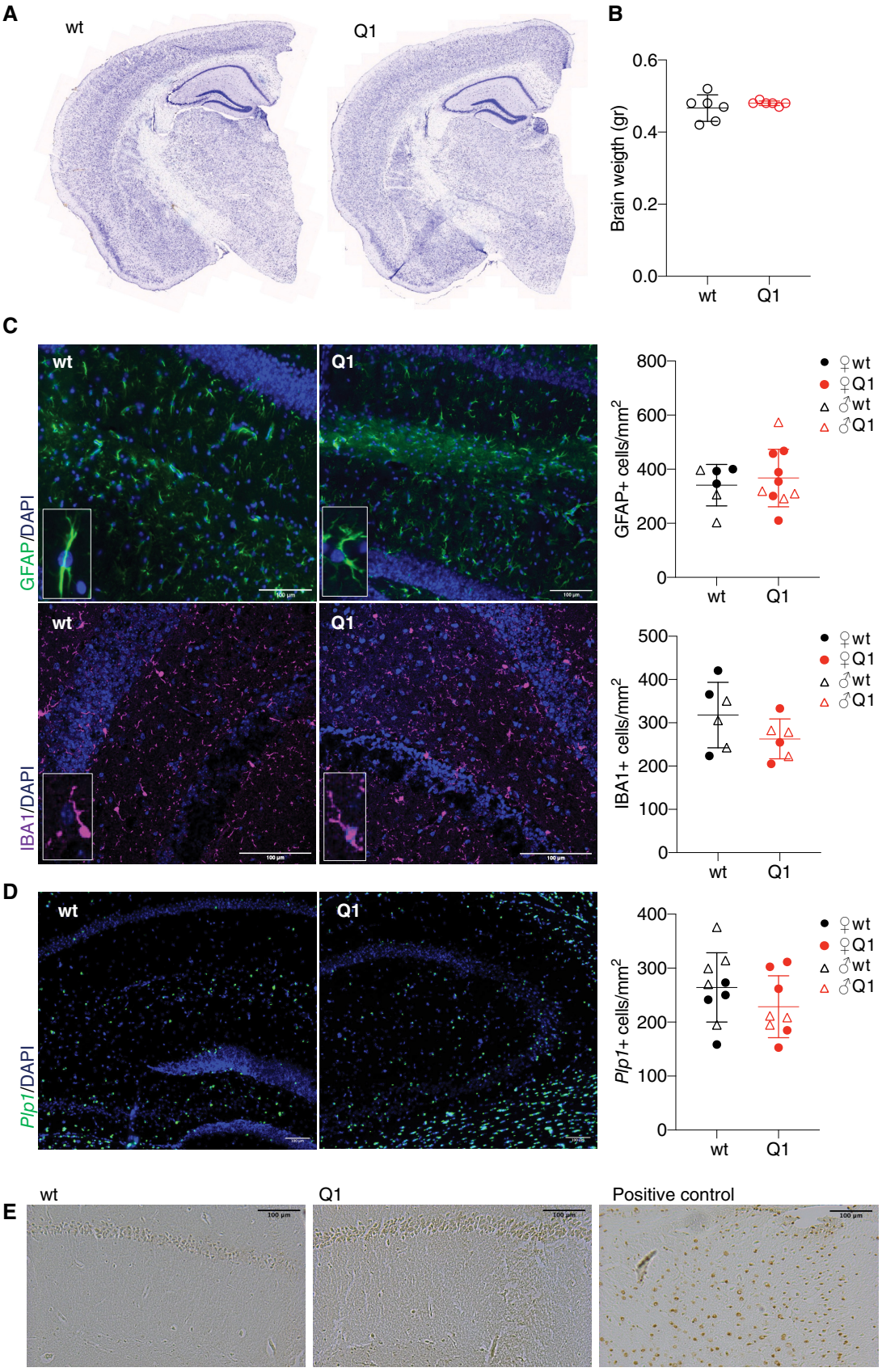

Figure EV2.

Figure EV3. Quantification of dendritic spines of dentate gyrus.

A Representative images of NeuN staining of hippocampal neurons from 8-month-old wt and Q1 mice. Red rectangles indicate magnified pictures shown in Fig 4C. Scale bar 500 μm.

B Representative images of Golgi-Cox-stained brain sections of hippocampal neurons from 8-month-old wt and Q1 mice. Red rectangles show the area considered for the measurements of dendritic spine density in (D and E) and of the dendrite length and Sholl analysis (main Fig 4E and F). Scale bar 2 mm.

C Examples of dendritic spine counting window. Scale bar 500 μm. The spines were counted manually in ImageJ.

D, E Density of dentate gyrus spines in wt and Q1 mouse hippocampi. Error bars represent ±SD; (n = 5). The spines of at least five dendrites were quantified for each replicate.

Data information: Q1, *Qtrt1* knockout mouse; wt, wild-type mouse.

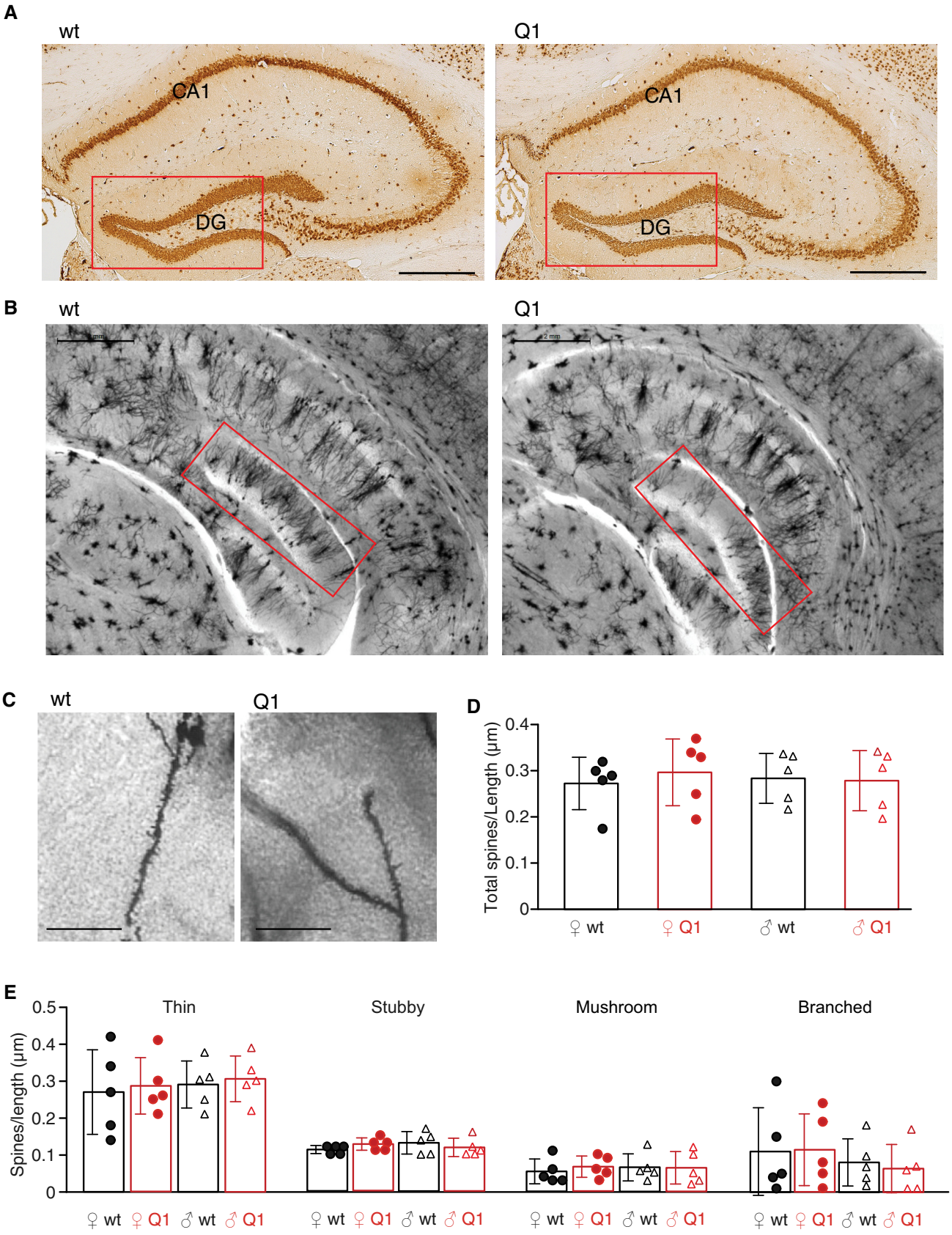

Figure EV3.

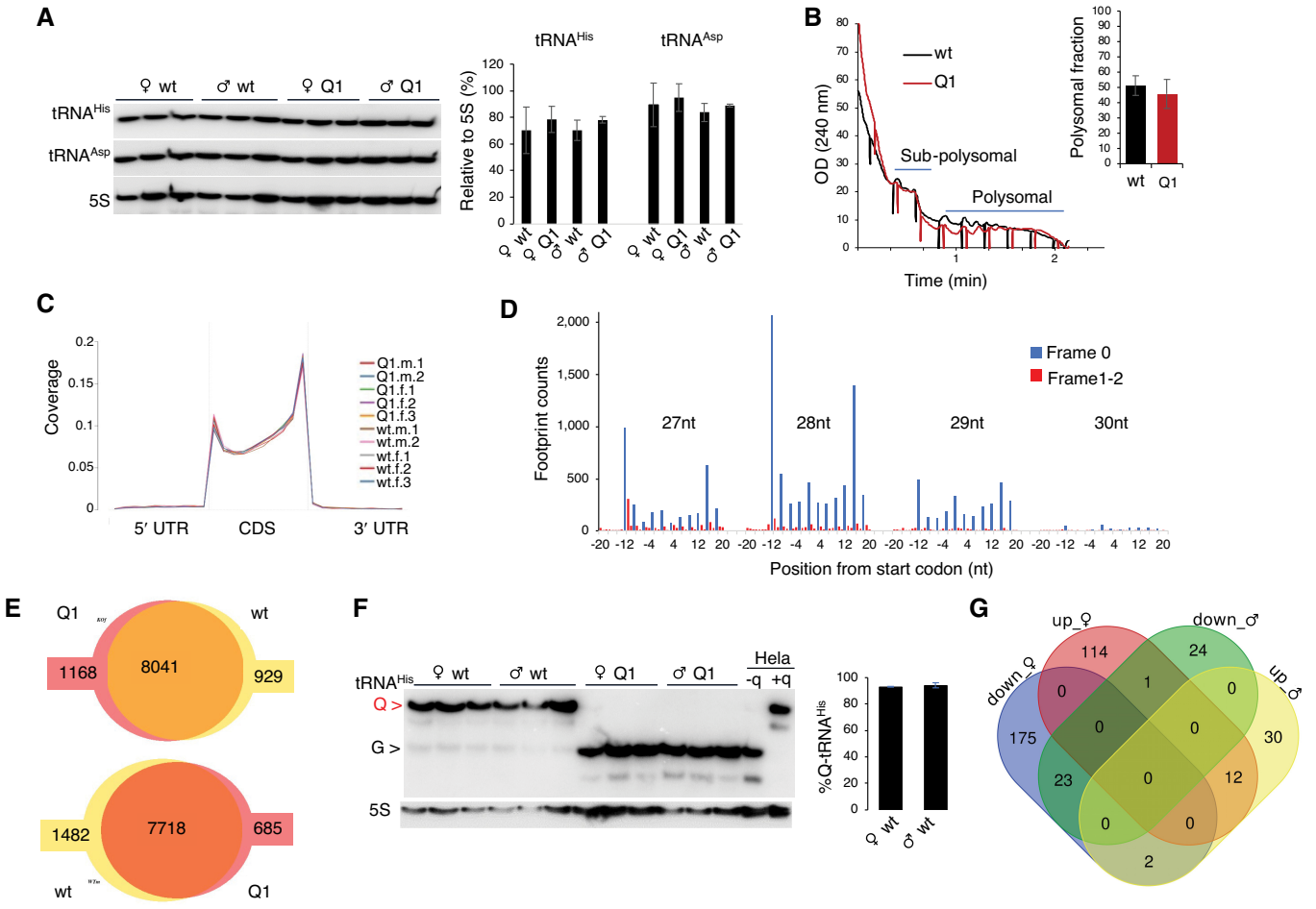

Figure EV4. Ribo-Seq quality control.

A The steady-state levels of $tRNA^{His}$ and $tRNA^{Asp}$ are not affected in the Q1 mice and between female and male hippocampi. 5S rRNA was used as a loading control. Data are represented as mean ± SD; n = 3 female and 3 male biological replicates.

B Representative polysome profiling tracks and quantification of polysomal fractions (wt: n = 2 male and 1 female, Q1: n = 2 male and 2 female) from hippocampi lysates of the 7- to 8-month-old mice. Data are represented as mean ± SD.

C Metagene plot of 27–30 mer ribosome footprints in all biological replicates.

D Periodicity bar plot. 27–30 nt footprints from female mouse (WT.f.2) are given as an example.

E Venn diagram showing the overlap between Q1 and wild-type mRNA-matching footprints in male (n = 2) and female (n = 3) mice.

F The Q-$tRNA^{His}$ level is similar between male and female mice. HeLa cell culture system was used for comparison. -q: serum-free medium, +q: serum-free medium supplemented with 20 nM queuine. 5S rRNA is shown as a loading control. Q-tRNA content was quantified by dividing the amount of Q-tRNA by total amount of detected tRNA. Data are represented as mean ± SD; n = 3 female and 3 male biological replicates.

G Venn diagram showing the overlap between RD dysregulated transcripts in males (n = 2) and females (n = 3).

Data information: CDS, coding sequence; G, Guanosine-tRNA; nt, nucleotide; Q, Queuosine-tRNA; Q1, *Qtrt1* knockout mouse; UTR, untranslated region; wt, wild-type mouse.
Source data are available online for this figure.

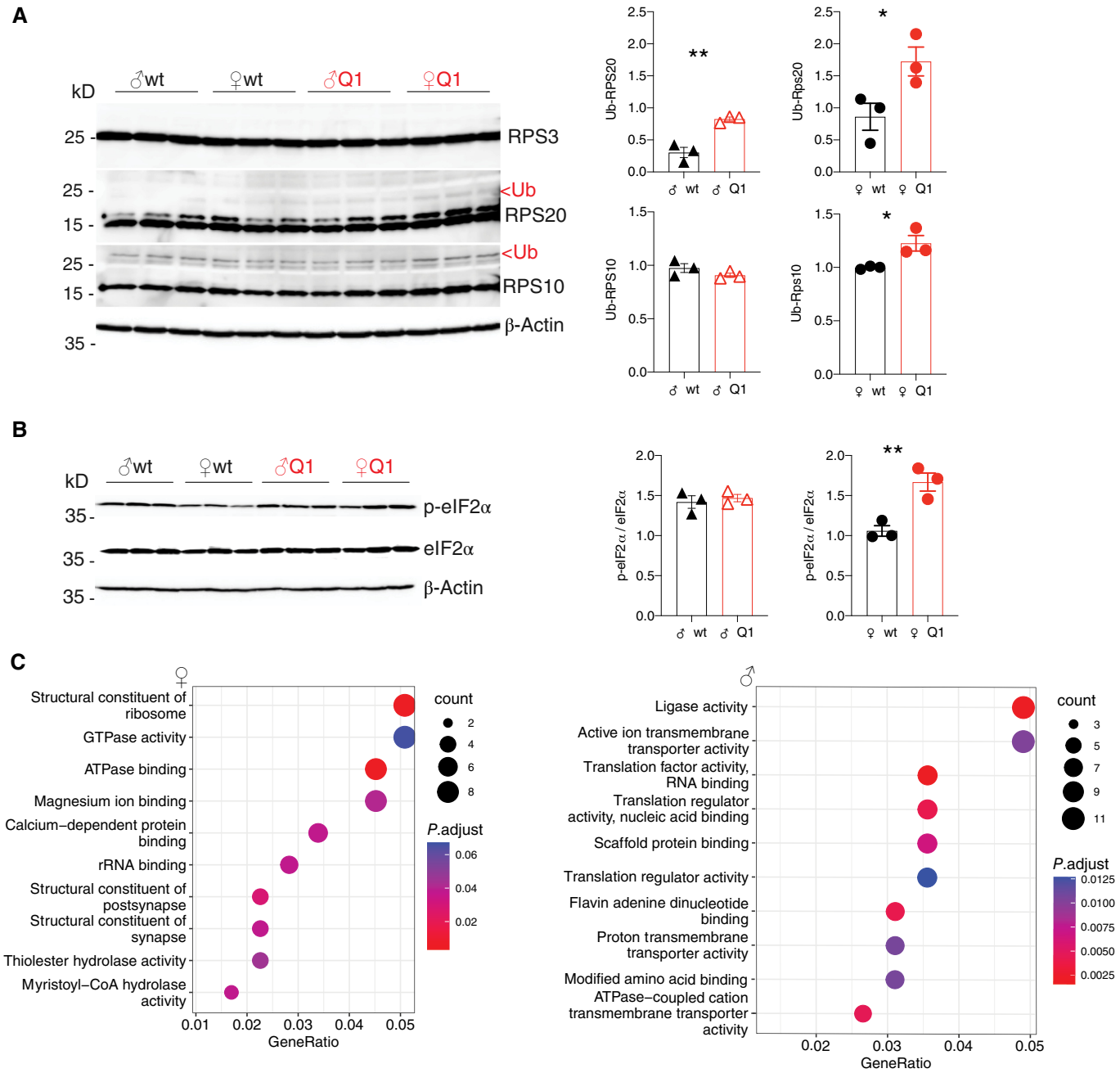

Figure EV5. The loss of Q-tRNA modification alters proteome in the adult hippocampus.

A Western blot analysis showing increased levels of ubiquitinylated RPS10 and RPS20 upon loss of Q in the 8-month-old hippocampi. RPS3 shows no detectable modifications. β-Actin was used as a loading control. The level of bands corresponding to ubiquitinylated RPS10 and RPS20 was quantified and the signal was normalized to β-Actin. Error bars represent ±SD (n = 6, 3 males and 3 females). *P-value < 0.05, two-tailed unpaired t-test.

B Western blot analysis showing increased levels of phosphorylated eIF2α upon loss of Q in the 8-month-old female Q1 liver. β-Actin and global eIF2α levels were used as loading controls. For the quantification of the level of eIF2α phosphorylation, the signal was normalized to total eIF2α. Error bars represent ±SD; (n = 6, 3 males and 3 females). **P-value < 0.01, two-tailed unpaired t-test.

C Gene ontology analysis of the deregulated proteins. The top 10 molecular functions are presented. Adjusted P-value was calculated using Benjamini–Hochberg method.

Data information: Q1, *Qtrt1* knockout mouse; P, proteome; wt, wild-type mouse.